Interaction of nitro compounds with radicals: a quantum chemical study

S. V. Zelentsov and I. V. Simdyanov*

N. I. Lobachevsky Nizhny Novgorod State University,
23 prosp. Gagarina, Nizhny Novgorod, 603950 Russian Federation.
Fax: +7 (831 2) 65 8592. E-mail: zelentsov@thermo.chem.unn.ru

Photoreduction of nitro compounds is accompanied by formation of various radical products that can react with the starting nitro compound, thus causing deviation of the decomposition kinetics from the first-order kinetics with respect to the nitro compound. The results of quantum chemical modeling of the reactions of nitro compounds with radicals and the pathways of further transformations of radical adducts formed in the reactions are presented.

Key words: photoreduction, nitro compound, nitrene—dioxygen complex, radical products, quantum chemical modeling, activation energy, thermal effect.

UV-Irradiation of a molecule of a nitro compound RNO_2 leads to its transition into excited state in which RNO_2 can undergo isomerization into nitroso oxide $^1RNOO^*$. These species are key intermediates of the photooxidation of aromatic azides[1] and the photoreduction of aromatic nitro compounds.[2] Their transformations have been documented.[1—4]

Scheme 1

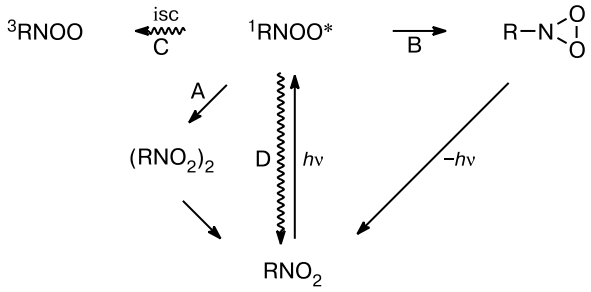

isc — intersystem crossing

Nitroso oxide can enter bimolecular reactions involving formation of, *e.g.*, dimers (route A)[1] as well as undergo a photoinduced rearrangement into *N*-dioxaziridine (route B)[1,4] and the intersystem crossing to triplet ^3RNOO (route C).[1,3,4] The triplet nitroso oxide is capable of abstracting a proton from hydrogen-containing molecules of the medium, thus forming *N*-hydroperoxyaminyl radical $RN^{\bullet}OOH$.[3]

$$^3RNOO + H{-}R' \xrightarrow[-\dot{R}']{} RN\dot{O}OH \xrightarrow[-\dot{O}H]{} RNO \qquad (1)$$

Reaction (1) results in the formation of considerable amount of radical products. A spin trap study[5] showed that the major trapped products are the radicals $^{\bullet}R'$ generated owing to proton abstraction from solvent molecules. We assumed[6] that radicals $^{\bullet}R'$ can react with molecules of the starting nitro compound, thus favoring an increase in the RNO_2 consumption rate and a shift of the consumption kinetics from the first-order kinetics toward a higher rate of reaction (2).

$$R{-}\overset{+}{N}(=O){-}O^- + \dot{R}' \longrightarrow R{-}N(\cdot){-}O{-}R' \qquad (2)$$

1

The contribution of bimolecular reaction (2) to the overall process of RNO_2 consumption strongly depends on the concentration of radicals. The efficiency of radical generation can be significantly improved by adding EtBr (efficient catalyst of intersystem crossing) to the reaction mixture.[7] In this case the formation of triplet nitroso oxide is no longer the limiting stage of the photoreduction of nitro compounds. The yield of this reaction becomes dependent on the chemical nature of hydrogen-containing molecules of the reaction medium, because an increase in the concentration of the radicals produced upon proton abstraction is followed by an increase in the contribution of reaction (2) to the overall consumption of the nitro compound.

The spin adduct **1** can then enter a number of reactions. The most probable transformations are as follows: the reaction involving regeneration of the starting radical and nitro compound (reverse reaction with respect to reaction (2)):

$$\mathbf{1} \longrightarrow R{-}\overset{+}{N}(=O){-}O^- + \dot{R}', \qquad (3)$$

reversible decomposition into a nitroso compound and a hydroxy-, alkoxy-, or aroxy radical:

$$\mathbf{1} \rightleftharpoons R{-}N{=}O + \dot{O}R', \qquad (4)$$

Published in Russian in *Izvestiya Akademii Nauk. Seriya Khimicheskaya,* No. 2, pp. 202—206, February, 2006.

and the decomposition into nitrite and a carbon-centered radical:

$$\mathbf{1} \rightleftharpoons R'-O-N=O + \dot{R}. \qquad (5)$$

The composition of the radical products present in the reaction mixture is determined by the competition of reactions (3)—(5).

The aim of this work was to check the assumption of additional channel of nitro compound consumption owing to the interaction with intermediate radicals and to assess the probabilities of reactions (3)—(5) by modern quantum chemical methods.

Calculation Procedure

Quantum chemical calculations were carried out in the framework of the density functional theory (DFT)[8,9] with the UB3LYP gradient hybrid functional[9] and the 6-31G* basis set. The S^2 parameter for the doublet state was in the range 0.75—0.79.

The energy effects of the reaction of formation of spin adducts RN(˙O)OR´ (reaction (2)) were calculated for R = R´ = H, Me, and Ph. For all compounds, full geometry optimization was performed. All stationary points localized were characterized by real vibrational frequencies.

The search for transition states (TS) of the decomposition reactions (3)—(5) of the spin adducts RN(˙O)OMe (R = H, Me, Ph) involved full geometry optimization including variation of the length of the bond chosen as the reaction coordinate (C—O, N—O, and C—N (C—H for R = H), respectively) with an increment of 0.01 nm. In the vicinity of the TS, full geometry optimization was performed again including variation of the length of the bond chosen as the reaction coordinate. IRC calculations carried out for each TS led to the expected reaction products and starting compounds.

The activation energies were calculated ignoring zero-point vibrational energies.

Calculations were carried out using the GAUSSIAN-94 program[10] at the Computer Assistance to Chemical Research Center of the Division of Chemistry and Materials Science, Russian Academy of Sciences (Zelinsky Institute of Organic Chemistry, Russian Academy of Sciences, Moscow).

Results and Discussion

The geometric parameters of the spin adducts R—N(O˙)O—Me (R = H, Me, Ph) are listed in Table 1 (atomic numbering scheme is shown in Fig. 1). Variation of the nature of the substituent R has little effect on the geometric parameters of the O(1)—N(2)—O(3)—C(4) fragment. The exception is the O(1)—N(2)—O(3)—C(4) dihedral angle equal to zero for R = Ph; this suggests stabilization of the NO_2 group due to involvement in the π-system of the aromatic ring.

The distribution of the spin density localized on the atoms and other structural fragments of the spin adducts is shown in Fig. 1. The spin density is mainly localized on the N(2) nitrogen atom and on the terminal oxygen atom, O(1). As should be expected, the total spin density

Table 1. Geometric parameters of spin adducts RN(˙O)OMe (R = H, Me, Ph) obtained from B3LYP/6-31G(d) calculations (atomic numbering scheme is shown in Fig. 1)

Parameter	R		
	H	Me	Ph*
Bond		*d*/nm	
O(1)—N(2)	0.1250	0.1252	0.1251
N(2)—O(3)	0.1442	0.1452	0.1420
O(3)—C(4)	0.1425	0.1424	0.1429
C(4)—H(6)	0.1092	0.1092	0.1091
C(4)—H(7)	0.1096	0.1096	0.1094
C(4)—H(8)	0.1094	0.1094	0.1094
N(2)—C(5)**	0.1028	0.1467	0.1396
Angle		ω/deg	
O(1)—N(2)—O(3)	120.3	118.5	120.0
O(1)—N(2)—C(5)**	118.6	120.0	126.2
N(2)—O(3)—C(4)	110.8	111.0	111.5
O(1)—N(2)—O(3)—C(4)	29.8	27.0	0.0

* The bond lengths and bond angles for benzene ring are not shown.

** At R = H, the atom No. 5 is the hydrogen atom.

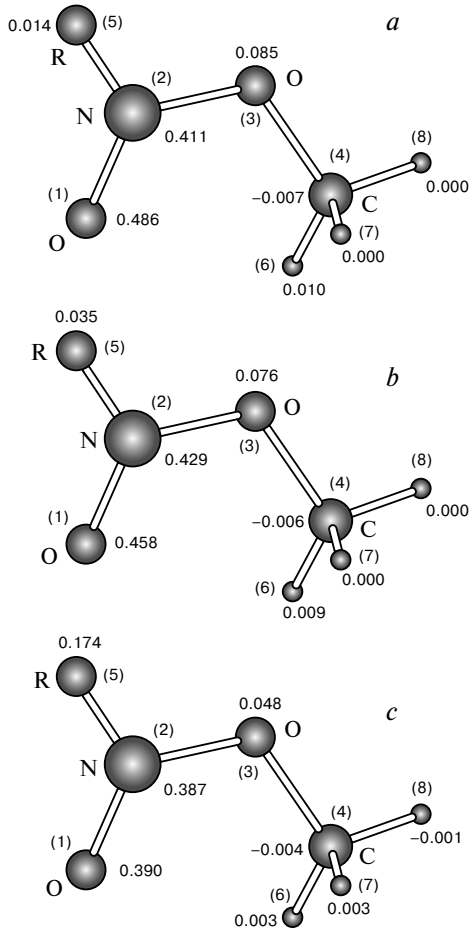

Fig. 1. Spin density distribution in spin adducts RN(˙O)OR´ at R´ = Me; R = H (*a*), Me (*b*), and Ph (*c*).

Table 2. Calculated thermal effects (ΔH_r) of reactions (2) (R, R′ = H, Me, Ph)

R′/R	$-\Delta H_r$/kJ mol^{-1}		
	H	Me	Ph
H	201.3	197.2	170.0
Me	128.0	122.0	126.1
Ph	203.1	164.9	165.8

on the N(2) and O(1) atoms decreases in the order R = H, Me, Ph while the total spin density on the substituent R simultaneously increases; this is most pronounced on going from R = Me to R = Ph. It was found that variation of the substituent R in the radical adduct **1** has little effect on the geometric parameters of the reaction center N(•O)O. Therefore, in order to reveal the effect of the substituent R′, we calculated the thermal effects of reaction (2). The results obtained are presented in Table 2; the least pronounced thermal effect was obtained for R′ = Me.

Table 3 lists the activation energies and thermal effects of reaction (3) at different R for R′ = Me. In Fig. 2 we present the profiles of the potential energy surfaces (PES) along the line of the C(4)—O(3) bond, which is the coordinate of reaction (3) for R′ = Me and R = H, Me, Ph. For R = H and Me, the activation energy (E_a) of the reaction is low, whereas for R = Ph one has E_a = 191.1 kJ mol^{-1}. It should be noted that in all cases reaction (3) is endothermic with a thermal effect, ΔH_r, of about 120 kJ mol^{-1} (see Fig. 2 and Table 3). Note that the nature of the substituent R has almost no effect on the reaction because R is far from the reaction center.

Table 3. Total energies (E_{total}) of starting compounds (SCs), transition states (TSs), and products (P) of reactions (3)—(5), which were used in calculations of activation energies (E_a) and thermal effects (ΔH_r) of these reactions (R = H, Me, Ph; R′ = Me)

R	$-E_{total}$(SC)	$-E_{total}$(TS)	$-E_{total}$(P)	E_a	ΔH_r
	a.u.			kJ mol^{-1}	
			Reaction (3)		
H	245.57380	245.51903	245.52523	146.2	128.1
Me	284.89391	284.84008	284.84762	141.5	121.8
Ph	476.63672	476.56414	476.58888	191.1	126.0
			Reaction (4)		
H	245.57380	—*	245.51834	0.0	146.2
Me	284.89391	—*	284.84457	0.0	130.2
Ph	476.63672	476.59077	476.59000	121.0	123.0
			Reaction (5)		
H	245.57380	245.50682	245.50823	176.4	173.0
Me	284.89391	284.84337	284.84457	133.1	125.6
Ph	476.63672	476.54898	476.56924	231.4	177.6

* No transition state.

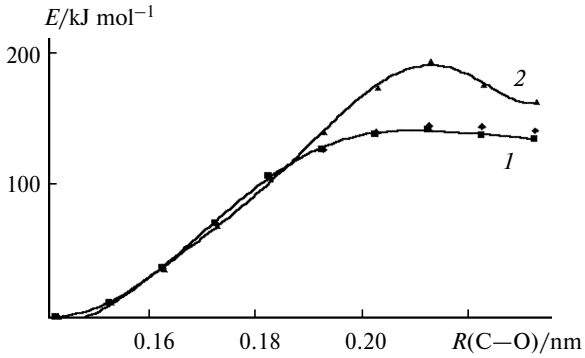

Fig. 2. PES profiles for reaction (3) of decomposition of spin adduct RN(•O)OR′ along the line of the C(3)—O(4) bond at R′ = Me; R = H, Me (*1*), and Ph (*2*).

For R′ = Me, the transition states of reaction (3) are characterized by one imaginary frequency equal to 410.5i (R = H), 401.2i (Me) and 278.2i (Ph) cm^{-1}. In all cases, this corresponds to infinite motion of methyl radical. The geometric parameters of the transition states are listed in Table 4. Similarly to the TS of reaction (4), in reaction (3) the O(1)—N(2)—O(3)—C(4) dihedral angle equals 0° for R = Ph, which suggests stabilization of electrons of the NO_2 group by the π-electron system of the aromatic ring.

The spin density on the O(1) and N(2) atoms of the TS of reaction (3) decreases in absolute value in the order R = H, Me, Ph (Fig. 3).

The second possible route of decomposition of the spin adduct **1** is the decomposition into a nitroso compound and a methoxyl radical. Fig. 4 presents the PES cross sections along the reaction coordinate (N—O bond)

Table 4. Geometric parameters of transition states of reaction (3) (R = H, Me, Ph; R′ = Me, atomic numbering scheme is shown in Fig. 1)

Parameter	R		
	H	Me	Ph*
Bond		*d*/nm	
O(1)—N(2)	0.1239	0.1242	0.1229
N(2)—O(3)	0.1258	0.1260	0.1245
O(3)—C(4)	0.2125	0.2124	0.2129
C(4)—H(6)	0.1082	0.1082	0.1082
C(4)—H(7)	0.1084	0.1084	0.1083
C(4)—H(8)	0.1083	0.1083	0.1082
N(2)—C(5)**	0.1035	0.1482	0.1471
Angle		ω/deg	
O(1)—N(2)—O(3)	126.6	124.1	124.5
O(1)—N(2)—C(5)**	117.4	118.3	117.9
N(2)—O(3)—C(4)	113.1	112.6	178.8
O(1)—N(2)—O(3)—C(4)	71.5	71.5	0.0

* The bond lengths and bond angles for benzene ring are not shown.

** At R = H, the atom No. 5 is the hydrogen atom.

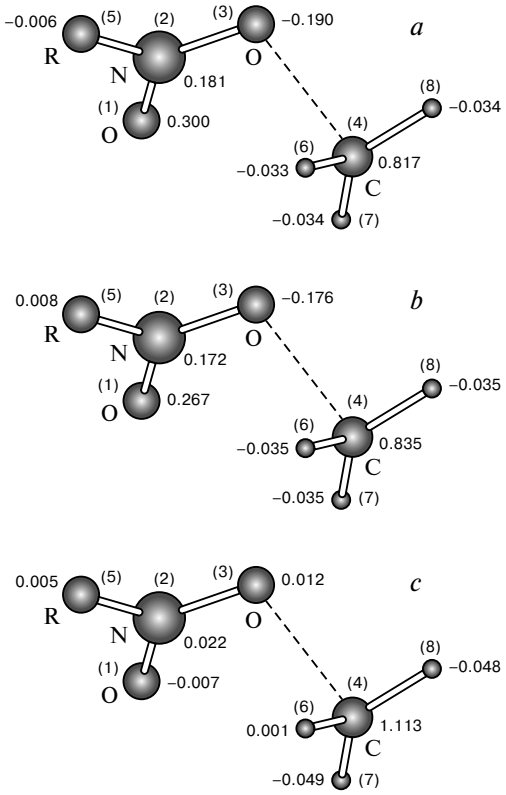

Fig. 3. Calculated spin density distribution in transition states of reaction (3) at R′ = Me; R = H (*a*), Me (*b*), Ph (*c*).

for reaction (4). According to calculations, the reaction proceeds barrierlessly with R = H and Me. Calculations for R = Ph revealed a local minimum at r(N(2)—O(3)) = 0.262 nm, which is due to formation of additional H-bonds between H atoms of the methoxyl radical and the nitroso group of nitrosobenzene (Fig. 5). Further increase in r(N(2)—O(3)) leads to barrierless decomposition of the intermediate complex into nitroso compound and methoxyl radical.

The activation energy and thermal effect calculations for reaction (4) with different R (see Table 3) showed that

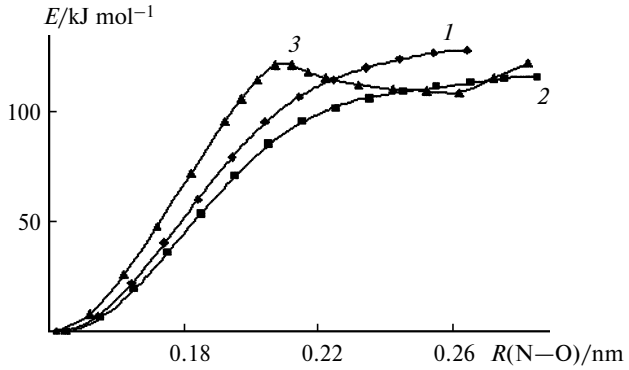

Fig. 4. PES profiles for reaction (4) along the reaction coordinate — line of the O(3)—N(2) bond at R′ = Me: R = H (*1*), Me (*2*), and Ph (*3*).

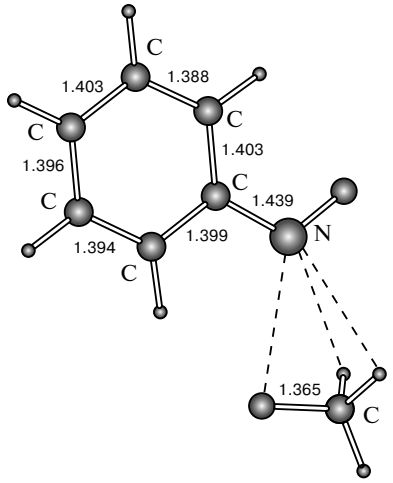

Fig. 5. Structure corresponding to local minimum in modeling of reaction (4); R = Ph and R′ = Me.

it is endothermic similarly to reaction (3) and its thermal effect decreases in the order R = H, Me, Ph. The reactions with R = H and Me proceed almost barrierlessly (see Fig. 4). The transition state of the reaction with R = Ph is characterized by one imaginary frequency of 1114.6i cm^{-1}.

The third possible route of decomposition of the spin adduct **1** involves cleavage of the N(2)—C(5) bond to give R′—O—N=O and ˙R. The calculated structures of the transition complexes of reactions (5) and the corresponding spin density distributions are shown in Fig. 6. According to calculations, at R = H and Me the spin density is almost completely localized on the leaving radical. Transition states of reaction (5) are characterized by imaginary

Table 5. Geometric parameters of transition states of reaction (5) (R = H, Me, Ph; R′ = Me, atomic numbering scheme is shown in Fig. 6)

Parameter	R		
	H	Me	Ph*
Bond		*d*/nm	
O(1)—N(2)	0.1191	0.1196	0.119
N(2)—O(3)	0.1399	0.1426	0.144
O(3)—C(4)	0.1438	0.1439	0.143
C(4)—H(6)	0.1090	0.1091	0.110
C(4)—H(7)	0.1094	0.1095	0.109
C(4)—H(8)	0.1094	0.1095	0.109
N(2)—C(5)**	0.2128	0.2367	0.215
Angle		ω/deg	
O(1)—N(2)—O(3)	114.7	114.2	113.9
O(1)—N(2)—C(5)**	117.2	112.6	106.9
N(2)—O(3)—C(4)	115.3	114.7	115.1
O(1)—N(2)—O(3)—C(4)	0.0	0.9	0.0

* The bond lengths and bond angles for benzene ring are not shown.

** At R = H, the atom No. 5 is the hydrogen atom.

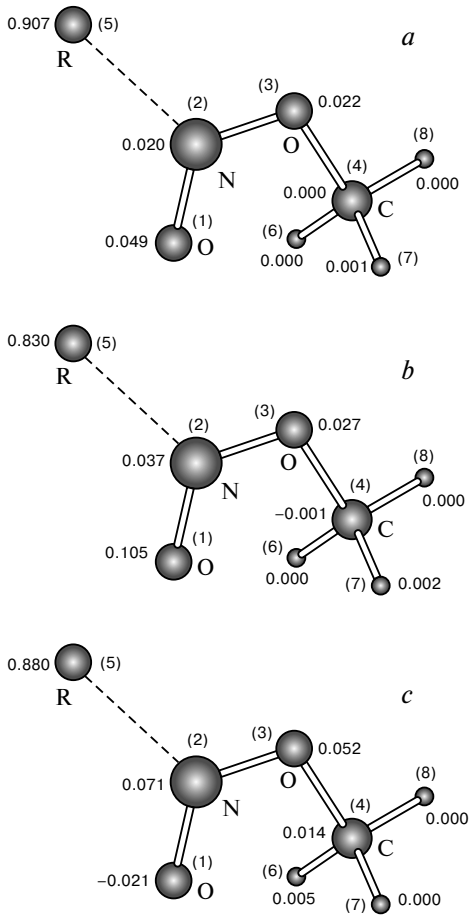

Fig. 6. Calculated spin density distribution in transition state of reaction (5). The reaction coordinate is the N(2)—C(5) bond for R = Me and Ph and the N(2)—H(5) bond for R = H (*a*), Me (*b*), and Ph (*c*); R′ = Me.

frequencies of 439.9i (R = H), 402.0i (Me), and 711.9i (Ph) cm^{-1}; the corresponding geometric parameters are listed in Table 5.

Figure 7 presents the PES sections along the coordinate of this reaction (C(5)—N(2) bond for R = Me and Ph and the H(5)—N(2) bond for R = H). Similarly to reaction (4), reaction (5) proceeds almost barrierlessly for R = H and Me; the energy barrier appears only for R = Ph.

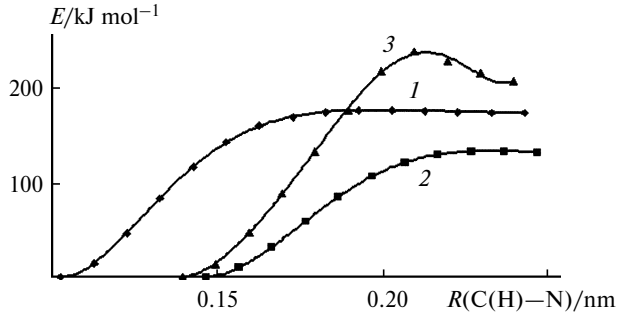

Fig. 7. PES profiles along the reaction coordinates calculated for reaction (5). The reaction coordinate is the C—N bond (R = Me, Ph) or the C—H bond (R = H); R′ = Me; R = H (*1*), Me (*2*), and Ph (*3*).

Table 3 lists the activation energies and thermal effects of reaction (5) calculated for different substituents R. As in the three preceding cases, the reactions are endothermic with the lowest E_a value obtained for R = Me.

Thus, our quantum chemical study showed that the nitro compounds readily react with radicals. The resultant spin adduct R—N(O•)O—R′ is quite stable, so the probability of its decomposition is low.

This work was financially supported by the Inter-Higher-School Scientific and Technological Program "Higher School Research and Development on Priority Avenues" (Project 203.02.05.003) and the "Universities of Russia" research program (Project UR 05.01.019).

References

1. J. S. Brinen and B. Singh, *J. Am. Chem. Soc.*, 1971, **93**, 6623.
2. A. A. Shchepalov, S. V. Zelentsov, and A. G. Razuvaev, *Izv. Akad. Nauk. Ser. Khim.*, 2001, 2239 [*Russ. Chem. Bull.*, 2001, **50**, 2346].
3. S. V. Zelentsov, N. V. Zelentsova, A. B. Zhezlov, and A. V. Oleinik, *Khim. Vys. Energ.*, 2000, **34**, 201 [*High Energy Chem.*, 2000, **34** (Engl. Transl.)].
4. T. Harder, P. Wessig, J. Bendig, and R. Stosser, *J. Am. Chem. Soc.*, 1999, **121**, 6580.
5. S. V. Zelentsov, N. V. Zelentsova, M. V. Kuznetsov, and I. V. Simdyanov, *Khim. Vys. Energ.*, 2004, **38**, 28 [*High Energy Chem.*, 2004, **38** (Engl. Transl.)].
6. I. V. Simdyanov and S. V. Zelentsov, *Tez. dokl. XI Mezhdunar. konf. po khimii organicheskikh i elementoorganicheskikh peroksidov (Moskva, 24—26 iyunya 2003)* [*Abstrs XIth Int. Conf. on Organic and Organoelement Peroxides (June 24—26, 2003, Moscow, Russia)*], Moscow, 2003, 208 (in Russian).
7. J. G. Calvert and J. N. Pitts, Jr., *Photochemistry*, Wiley, New York, 1966.
8. W. Kohn and L. J. Sham, *Phys. Rev.*, *A*, 1965, **140**, 1133.
9. A. Pople, P. M. V. Gill, and B. G. Johnson, *Chem. Phys. Lett.*, 1992, **199**, 557.
10. M. J. Frisch, G. W. Trucks, H. B. Schlegel, P. M. W. Gill, B. G. Johnson, M. A. Robb, J. R. Cheeseman, T. A. Keith, G. A. Petersson, J. A. Montgomery, K. Raghavachari, M. A. Al-Laham, V. G. Zakrzewski, J. V. Ortiz, J. B. Foresman, J. Cioslowski, B. B. Stefanov, A. Nanayakkara, M. Challacombe, C. Y. Peng, P. Y. Ayala, W. Chen, M. W. Wong, J. L. Andres, E. S. Replogle, R. Gomperts, R. L. Martin, D. J. Fox, J. S. Binkley, D. J. Defrees, J. Baker, J. P. Stewart, M. Head-Gordon, C. Gonzalez, and J. A. Pople, *GAUSSIAN-94*, Gaussian, Inc., Pittsburgh (PA), 1995.

Received September 21, 2004;
in revised form February 2, 2005